

OPEN

A novel *de novo* variant of *GABRA1* causes increased sensitivity for GABA *in vitro*

Friederike Steudle¹, Sabah Rehman², Konstantina Bampali^{1,2*}, Xenia Simeone², Zsofia Rona³, Erwin Hauser³, Wolfgang M. Schmidt⁴, Petra Scholze¹ & Margot Ernst^{1,2}

The *GABRA1* gene encodes one of the most conserved and highly expressed subunits of the GABA_A receptor family. Variants in this gene are causatively implicated in different forms of epilepsy and also more severe epilepsy-related neurodevelopmental syndromes. Here we study functional consequences of a novel *de novo* missense *GABRA1* variant, p.(Ala332Val), identified through exome sequencing in an individual affected by early-onset syndromic epileptic encephalopathy. The variant is localised within the transmembrane domain helix 3 (TM3) and *in silico* prediction algorithms suggested this variant to be likely pathogenic. *In vitro* assessment revealed unchanged protein levels, regular assembly and forward trafficking to the cell surface. On the functional level a significant left shift of the apparent GABA potency in two-electrode voltage clamp electrophysiology experiments was observed, as well as changes in the extent of desensitization. Additionally, apparent diazepam potency was left shifted in radioligand displacement assays. During prenatal development mainly alpha2/3 subunits are expressed, whereas after birth a switch to alpha1 occurs. The expression of alpha1 in humans is upregulated during the first years. Thus, the molecular change of function reported here supports pathogenicity and could explain early-onset of seizures in the affected individual.

Gamma-aminobutyric acid (GABA) is a secreted transmitter that transduces signals from cell to cell by binding to membrane bound GABA receptors. Binding of GABA to GABA_A receptors opens an ion channel, allowing chloride or hydrogencarbonate ions to pass and thereby changing the membrane potential. While playing many roles in a wide range of tissues, the family of GABA_A receptors is most studied as central nervous system mediator of fast GABA-ergic neurotransmission^{1,2,3}.

GABA_A receptors are either homopentamers or heteropentamers composed of up to four different subunits. Heteropentamers are assembled from a pool of 19 different subunits producing a large variety of receptor subtypes^{1,4-6}.

The GABA system is involved in embryonic neurodevelopment⁷⁻⁹. In rodents, the GABA system can be detected as early as E12 and evolves before the glutamatergic system⁹. GABA has multiple functions during neurodevelopment, such as regulating neuronal cell proliferation, maturation and migration^{8,9}. It exerts excitatory responses as well as trophic effects during prenatal development serving essential functions during neurogenesis². During birth, maternal oxytocin triggers a switch in GABAergic function from excitatory to inhibitory action in the newborn¹⁰. This is accompanied by a switch in subunit expression. The 19 subunits differ in their developmental spatio-temporal expression. Different cell types express very specific GABA_A receptor genes during defined time-points of development. The main GABA_A receptor population in the neonatal brain is thought to contain two α 2/3 subunits together with two β 2/3 subunits and a γ 2 subunit. The expression of α 1 is very low in pre- and perinatal rodent brain, but it increases dramatically after birth in all brain regions^{6,11-13}. In the adult mammalian brain, α 1 contributes to the majority of GABA_A receptors¹¹.

In humans, the upregulation of *GABRA1* expression after birth was shown to occur over the first postnatal years^{14,15}. It is highly expressed during adulthood in mammalian species and contributes to multiple different receptor subtypes^{1,11,14,16}. These receptor subtypes include synaptic ones, such as the highly expressed

¹Department of Pathobiology of the Nervous System, Center for Brain Research, Medical University Vienna, Vienna, Austria. ²Department of Molecular Neurosciences, Center for Brain Research, Medical University Vienna, Vienna, Austria. ³Landeskrankenhaus Thermenregion Mödling, Department of Pediatrics, Mödling, Austria. ⁴Neuromuscular Research Department, Center for Anatomy and Cell Biology, Medical University of Vienna, Vienna, Austria. ⁵These authors contributed equally: Friederike Steudle and Sabah Rehman. *email: konstantina.bampali@meduniwien.ac.at

benzodiazepine sensitive $\alpha 1\beta\gamma 2$ GABA_A receptors as well as extrasynaptic ones like $\alpha 1\beta$ binary and $\alpha 1\beta\delta$ receptors. GABA_A receptors are members of the superfamily of Cys-loop receptors. Structurally, each subunit consists of three domains: the extracellular domain (ECD) is located at the N-terminal end. This domain is followed by four transmembrane segments (helices TM1–4), forming a four helix bundle, the transmembrane domain (TMD), of which the TM2 helices form the ion pore. An intracellular domain (ICD, sometimes called “loop”) connects TM3 and TM4. Multiple ligand binding pockets exist within subunits and at the interfaces between neighboring subunits. In these pockets, different types of ortho- and allosteric ligands, including the agonist GABA, and modulators such as neurosteroids can bind¹⁷. For $\alpha 1$, the ECD contributes to the GABA binding site at the complementary face and to the benzodiazepine binding site at the principal face if the complementary neighbour is a γ subunit.

Genetic variants in genes encoding for GABA_A receptor subunits are widespread. Many of them seem to be naturally occurring polymorphisms, which do not cause any specific phenotype. Other variants are disease associated and are widely studied in brain-related disorders. This includes pathogenic *GABRA1* variants causing susceptibility to idiopathic generalized epilepsy (EIG13, OMIM 611136) or more severe epilepsy-related neurodevelopmental syndromes (e.g. early infantile epileptic encephalopathy, EIEE19; OMIM 615744)¹⁸.

The first link between a *GABRA1* variant and epilepsy was reported in 2002 as missense variant, NM_000806.5:c.965C > A p.(Ala322Asp), causing an amino acid exchange of a highly conserved alanine residue to aspartate in TM3 (A322D)^{19,20}. In 2006 another variant within TM3 was identified: a frame-shift causing single-base deletion in *GABRA1* (NM_000806.5:c.975delC p.(Ser326Glnfs*3)) associated with childhood absence epilepsy^{20,21}. Since then, more than 30 different variants, the vast majority of which are missense variants, have been identified in association with different forms of epilepsy or epilepsy-related syndromes²².

In vitro experiments indicate that many GABA_A receptors containing mutated $\alpha 1$ subunits often exhibit a lower sensitivity for GABA and reduced current amplitudes. This suggests a decrease in inhibitory activity and therefore increased susceptibility to seizures *in vivo*²². The reduction of GABA evoked currents can be due to different mechanisms, such as improper folding (A322D in TM3 inhibits transmembrane helix formation), changed receptor trafficking leading to retention in the endoplasmic reticulum (ER) and ER associated degradation (caused by the frame-shift S326fs328*) or nonsense mediated mRNA decay^{20,21,23}.

Here, we report the identification and *in vitro* characterization of a novel *de novo* variant in an individual affected by a severe early-onset epilepsy-related neurodevelopmental syndrome.

Results

Clinical data and genetic analysis. The affected individual, a 13 year old boy, was initially diagnosed with early-onset refractory seizures, and neurodevelopmental retardation. Currently, he has muscle hypotonia and severe psychomotor impairment. His facial features are dysmorphic (with brachycephaly and microcephaly). He needs percutaneous endoscopic gastrostomy (PEG) feeding since the age of 5 years.

The affected individual was born at 39 + 3 weeks of gestation (spontaneous delivery) to healthy parents of Chechen descent with unremarkable family history. The first epileptic seizure was observed at the age of 2 ½ months. At the age of 18 months, he was diagnosed with cryptogenic focal epilepsy with complex focal seizures, severe developmental retardation, and optic atrophy. At this age, he presented with almost no psychomotor development. Most medications failed to control seizures or had severe side effects. Currently, seizures are under control with topiramate, pregabalin and lamotrigine.

On MRI at the age of 2 ½ years, there was thinning of the *corpus callosum* as well as reduction of gray and white matter with increased ventricle and subarachnoid liquor spaces. A follow-up MRI at the age of 5 ½ years revealed cerebral atrophy, especially in the frontal and temporal regions (for detailed clinical history see Supplementary Complete Clinical Information, as well as Supplementary Table S1, Supplementary Figs. S2 and S3).

Exome sequencing was performed in 2014 from a DNA sample isolated from peripheral blood of the affected individual. Libraries were constructed using Agilent All Exon V5 enrichment and next-generation sequencing (100 bp paired-end) was performed using the Illumina HiSeq technology. Within the targeted coding exons, the average depth of coverage was 60-fold with 90% of target sequence covered at least 10-fold. Variant calling in genes known to be causatively related to epileptic encephalopathies revealed a novel missense variant located in exon 10 of the *GABRA1* (gamma-aminobutyric acid type A receptor alpha1 subunit) gene: c.995C > T p.(Ala332Val). The variant introduces an amino acid exchange of a highly conserved alanine residue to valine in TM3 (A332V) and is not listed as rare minor allele in reference datasets like gnomAD²⁴. *In silico* prediction using different algorithms, such as MutationTaster and CADD, indicated a high probability of pathogenicity^{25–27}. While conventional DNA sequencing confirmed the presence of the variant in the affected individual, it was shown to be absent in DNA isolated from both parents, leading to a genetic diagnosis compatible with early infantile epileptic encephalopathy, caused by a *de novo* missense variant in *GABRA1*.

Structural analysis and localisation of the variant. Disease associated variants are found in all three domains of the $\alpha 1$ protein, without any tendency to cluster in any particular region²². The $\alpha 1$ variant A332V described here is located in TM3 near the subunit interface. Two other missense variants associated with epilepsy have been also identified within this helix (A322D and the frame-shift S326fs328*). The TM3 is highly conserved between different species (see Fig. 1d) and especially the position 332 is also highly conserved between different subunits (Supplementary Fig. S4). This helix is part of a subunit-subunit interface. Even a rather conservative exchange in this highly conserved position is expected to impact on protein function.

***In vitro* expression, fluorescence western blot and immunostaining.** Several studies reported that mutations in GABA_A receptor subunits can impair cellular processes such as protein trafficking and expression¹⁸.

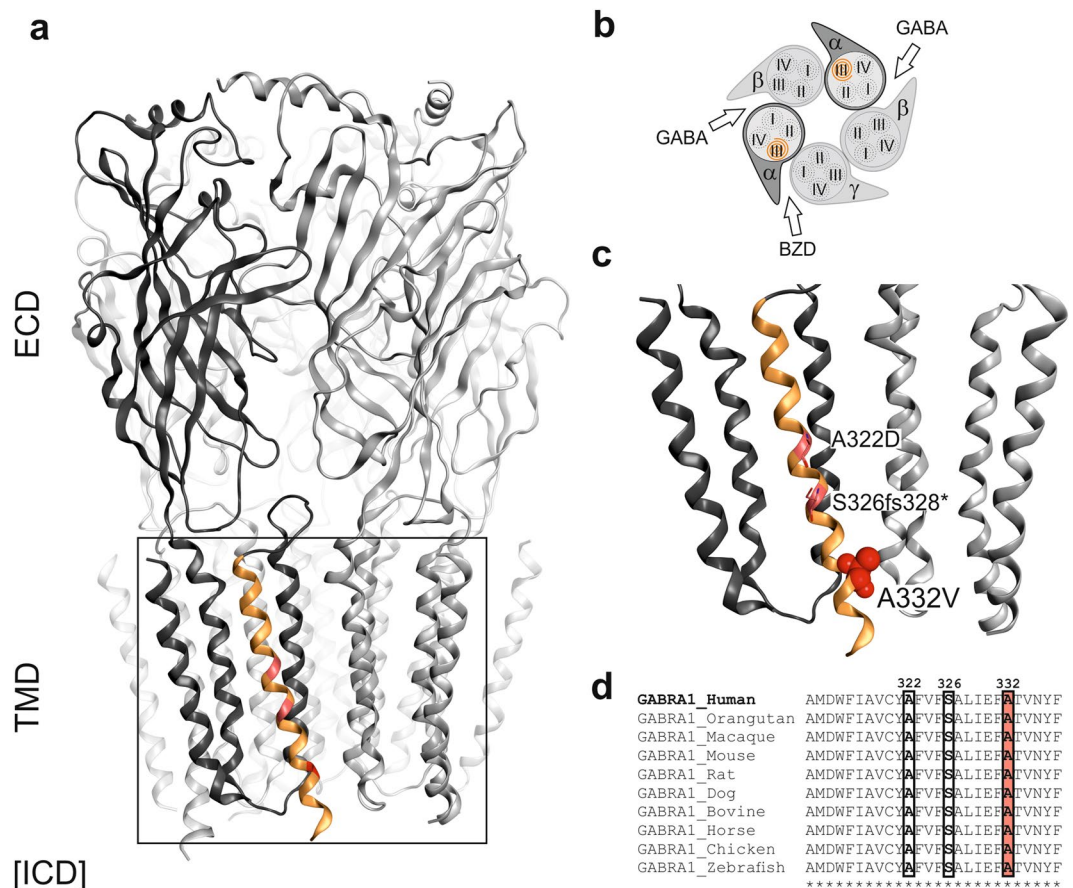


Figure 1. GABA_A receptor structure highlighting the A332V *de novo* variant. Panel (a) depicts an $\alpha 1\beta 3\gamma 2$ GABA_A receptor (the cryo-EM structure with PDB ID 6HUP⁴⁷). The schematic representation of the pentamer in panel (b) depicts a canonical $\alpha 1\beta 3\gamma 2$ receptor consisting of two α , two β and one γ subunit, where the TMD helices are numbered 1–4 (TM3 is highlighted). The binding sites for GABA and benzodiazepines (BZD) are indicated by arrows. Panel (c) shows a detailed view of the TMD region (M3 helix) where A332V, as well as A322D and S326fs328* are located. A332 is shown in a red atom view representation. In panel (d), a partial sequence alignment highlighting the 3 variants in TM3 of GABA_A receptor $\alpha 1$ subunit in humans with $\alpha 1$ subunit in other species, shows the levels of conservation (highlighted in red the high conservation of the A332 among the different species).

We examined the protein levels and cellular localization of the mutated GABA_A receptor in transfected HEK293 cells. As $\alpha 1\beta 3\gamma 2$ receptors are highly expressed in the brain, we studied this subtype in the HEK293 cells.

We used western blot analysis in order to estimate the protein expression levels of mutated and wild-type receptors. Due to the membrane preparation method it was not possible to differentiate in the western blot between surface and intracellular receptors.

As shown in Fig. 2a, we did not observe a significant difference between total wild-type and mutant $\alpha 1$ protein expression level ($p = 0.45$). This indicates that the mutated subunit is expressed at a similar level as the wild-type subunit.

Because in western blot no difference in total protein was detected we performed an immunostaining on transfected HEK293 cells to see if the cellular distribution of mutated and wild-type protein is similar. The results showed that wild-type and mutated $\alpha 1$ subunits can be detected at the cell surface to a similar amount and no significant intracellular staining was observed (see Fig. 2c).

Radioligand displacement assays. Benzodiazepines bind in the ECD between $\alpha 1$ and $\gamma 2$ subunits²⁸. Therefore, radioligand displacement assays with diazepam can be used to assess receptor assembly. We used $\alpha 1\beta 3\gamma 2$ transfected HEK293 cells with wild-type or mutated $\alpha 1$ and displaced 3H-flunitrazepam with varying concentrations of diazepam (Supplementary Fig. S5).

Radioligand binding was observed in both wild-type and mutated receptors, thus it appears that the mutated subunit is inserted in the receptor next to the $\gamma 2$ subunit as is the case for the $\alpha 1$ subunit in wild-type receptors. The calculated IC₅₀ values differed significantly ($p = 0.003$) between wild-type and mutated receptors (33 and 23 nM, respectively, Fig. 3). The variant seems to increase the affinity of diazepam to the receptor.

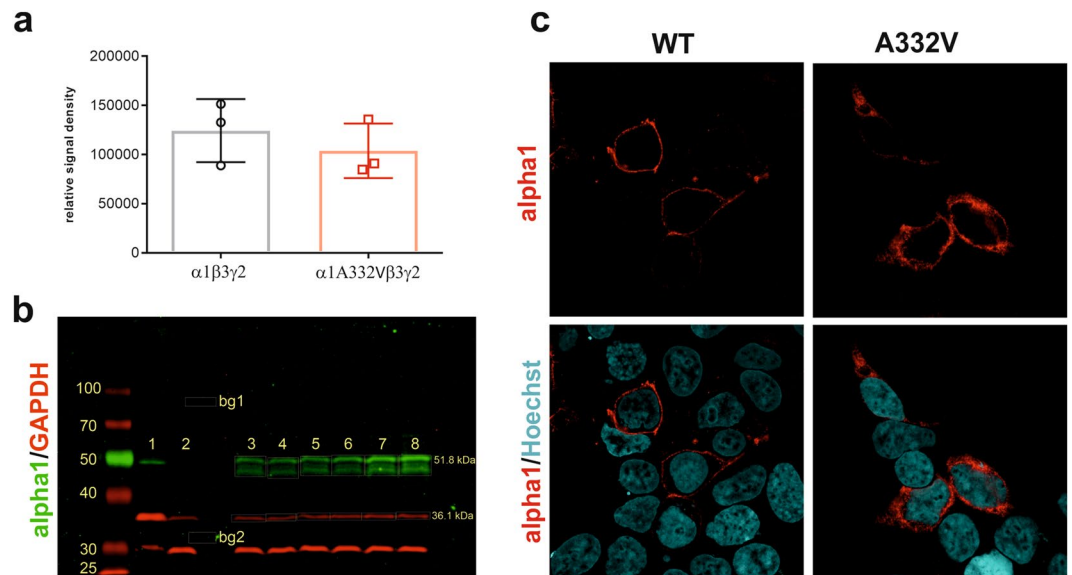


Figure 2. Protein expression of $\alpha 1$ in HEK293 cells. **(a)** Expression of total $\alpha 1$ protein was detected in HEK293 cells transfected with wild-type or mutant human $\alpha 1\beta 3\gamma 2$ cDNAs (ratio 1:1:5). Protein levels were normalised to GAPDH expression. **(b)** Representative western blot analysis ($n = 3$). 1: 20 μg mouse Hippocampus, 2: 20 μl untransfected HEK293 cells, 3–5: 20 μl HEK293 $\alpha 1\beta 3\gamma 2$, 6–8: 20 μl HEK293 $\alpha 1\beta 3\gamma 2$; bg1: background signal for green channel ($\alpha 1$), bg2: background signal for red channel (GAPDH). **(c)** Immunostaining of surface $\alpha 1$ expression (red). Both mutated and wild-type subunits appear at cell surfaces when co-expressed with $\beta 3$ and $\gamma 2$ subunits.

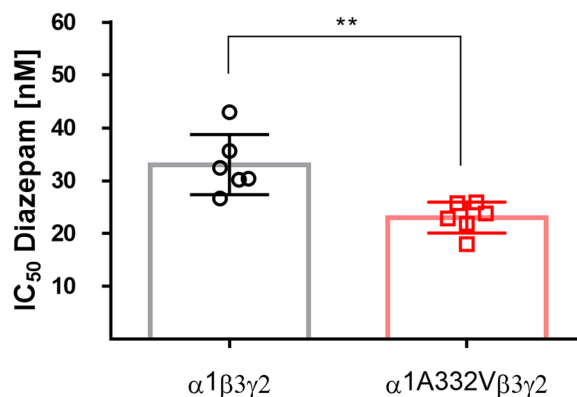


Figure 3. ^3H -flunitrazepam displacement in transfected HEK293 cells. ^3H -flunitrazepam displacement with increasing concentrations of diazepam was performed in HEK293 cells transfected with human $\alpha 1\beta 3\gamma 2$ cDNA with either wild-type $\alpha 1$ or mutant $\alpha 1\text{A}332\text{V}$. Values depict mean \pm SEM from six individual experiments. IC_{50} values for $\alpha 1\beta 3\gamma 2$ and for $\alpha 1\text{A}332\text{V}\beta 3\gamma 2$ are 33 nM and 23 nM, respectively. Statistically significant differences were determined by two-tailed students t -test, where $p < 0.05$; $**p < 0.01$.

Functional (two-electrode voltage clamp electrophysiology) data. Upon agonist binding to the ECD and activation of the GABA_A receptor, conformational changes occur that lead to channel opening. In order to assess whether the variant can have an impact on agonist effects, we expressed recombinant receptors containing human $\alpha 1\text{A}332\text{V}\beta 3$ or $\alpha 1\beta 3$ in *Xenopus laevis* oocytes either alone or in combination with $\gamma 2$, corresponding to an extrasynaptic and a synaptic subunit combination. After protein expression, we recorded whole cell GABA-induced currents with two-electrode voltage clamp electrophysiology. GABA dose response curves revealed a significant left shift (Fig. 4a,b). Interestingly, GABA activates $\alpha 1\text{A}332\text{V}\beta 3$ receptors with higher potency than wild-type receptors inducing effects already at nanomolar range (13% of maximum current at 100 nM) with EC_{50} values of 6.8 μM for wild-type receptors and 0.5 μM for mutated receptors (Fig. 4a,c). We also compared GABA dose response curves of $\alpha 1\beta 3\gamma 2$ with $\alpha 1\text{A}332\text{V}\beta 3\gamma 2$ receptors and also observed a significant left shift of the curve with EC_{50} values of 20.8 μM and 3.6 μM , respectively (Fig. 4b,d). To ensure the incorporation of the $\gamma 2$ subunit, we tested if $\gamma 2$ -containing receptors are sufficiently modulated by diazepam ($\sim 200\%$ at 1 μM diazepam). The relative populations of $\alpha 1\beta 3$ receptors and $\alpha 1\beta 3\gamma 2$ receptors cannot be quantified readily, but both the diazepam modulation and the different trace characteristics (Fig. 4e–h) demonstrate that the cells

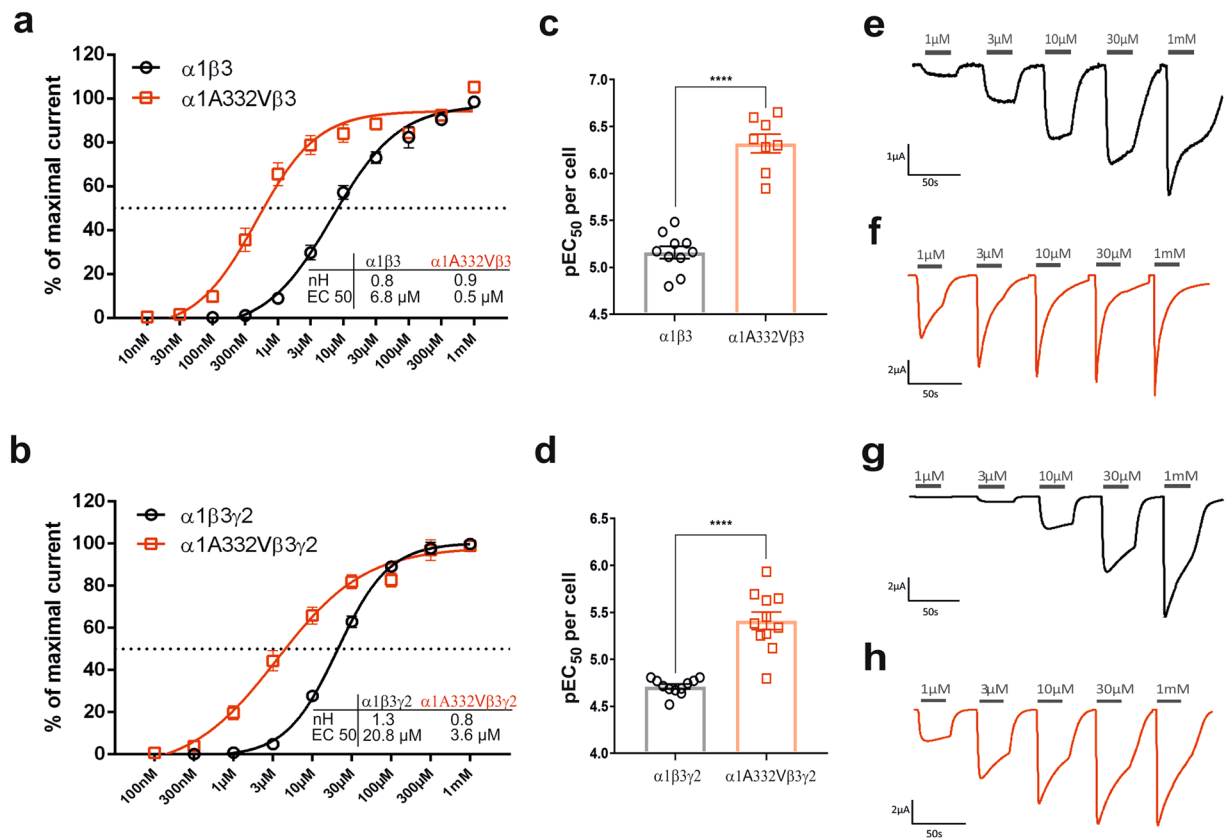


Figure 4. GABA dose response relationships in wild-type and mutated receptors. **(a,b)** GABA dose response curves of all four wild-type and mutated receptors. Data were fitted to a sigmoidal dose response with a variable slope and points are depicted as mean \pm SEM. Each data point represents experiments from $n = 7$ –12 oocytes from ≥ 2 batches. **(c,d)** The column graphs depict the pEC₅₀ values of $\alpha 1\text{A}332\text{V}\beta 3$, $\alpha 1\beta 3$, $\alpha 1\text{A}332\text{V}\beta 3\gamma 2$ and $\alpha 1\beta 3\gamma 2$ receptors obtained by fitting data of each cell individually. Statistically significant differences were determined by two-tailed students *t*-test, where $p < 0.05$; **** $p < 0.0001$. **(e,f)** Representative traces from electrophysiological recordings in $\alpha 1\beta 3$ **(e)** and $\alpha 1\text{A}332\text{V}\beta 3$ **(f)** receptors. **(g,h)** Representative traces from electrophysiological recordings in $\alpha 1\beta 3\gamma 2$ **(g)** and $\alpha 1\text{A}332\text{V}\beta 3\gamma 2$ **(h)** receptors.

express a sufficient amount of the ternary receptor. Moreover, absolute currents elicited by 1 mM GABA are significantly higher in $\alpha 1\beta 3\gamma 2$ compared to $\alpha 1\text{A}332\text{V}\beta 3\gamma 2$ receptors, whereas no statistically significant difference was observed between $\alpha 1\beta 3$ and $\alpha 1\text{A}332\text{V}\beta 3$ (Supplementary Fig. S6).

We next determined whether the variant changed the maximum efficacy of GABA by estimating the maximum open probability of GABA similar to previous studies²⁹. As shown in previous studies, the endogenous agonist GABA cannot activate the receptors to their maximal obtainable open-state probability ($P_{O(\max)}$)³⁰. Measuring the maximal efficacy of GABA in presence of an allosteric modulator is an established pharmacological method of estimating $P_{O(\max)}$, and is utilised in the absence of single-channel recordings^{30–32}. This technique enables us to determine whether the variant changes these intrinsic activation properties of the receptor.

We thus compared the Est. $P_{O(\max)}$ at $\alpha 1\text{A}332\text{V}\beta 3\gamma 2$ and $\alpha 1\beta 3\gamma 2$ receptors (Fig. 5a,b). We expected, as observed previously, that the co-application of GABA with etomidate and diazepam would open the receptors with a high probability²⁹. Therefore, we applied 3 mM GABA as a reference at $\alpha 1\text{A}332\text{V}\beta 3\gamma 2$ and $\alpha 1\beta 3\gamma 2$ receptors and then co-applied 10 mM GABA with 3 μM etomidate and 1 μM diazepam (Fig. 5a,b). This was performed in order to shift as many receptors as possible to the open state. A high Est. $P_{O(\max)}$ close to 1 was observed at both wild-type and mutated receptors with no significant difference. Next, we similarly applied 3 mM GABA as a reference at $\alpha 1\text{A}332\text{V}\beta 3$ and $\alpha 1\beta 3$ receptors and then co-applied 10 mM GABA with 3 μM etomidate and 10 μM LAU 176 (Fig. 5c,d). LAU 176 is an established, highly efficacious, positive allosteric modulator of $\alpha 1\beta 3$ receptors, acting primarily via the extracellular domain^{33,34}. We observed a significant difference between wild-type and mutated receptors, with the later resulting in a higher Est. $P_{O(\max)}$ (Fig. 5c,d).

To obtain more insight into the impact of $\alpha 1\text{A}332\text{V}$ on the receptor properties, we analysed the extent of desensitization in wild-type and mutated receptors at 1 μM , 30 μM and 1 mM GABA. $\alpha 1\text{A}332\text{V}\beta 3$ receptors exhibited a significantly more pronounced desensitization with 40% at 1 μM GABA and about 60% at 30 μM and 1 mM GABA compared to wild-type receptors (Fig. 6). Similarly, the extent of desensitization differed significantly in $\alpha 1\text{A}332\text{V}\beta 3\gamma 2$ at 1 μM and 30 μM GABA, however, at 1 mM GABA there is no difference in the extent of desensitization between $\alpha 1\text{A}332\text{V}\beta 3\gamma 2$ and $\alpha 1\beta 3\gamma 2$ (Fig. 6c).

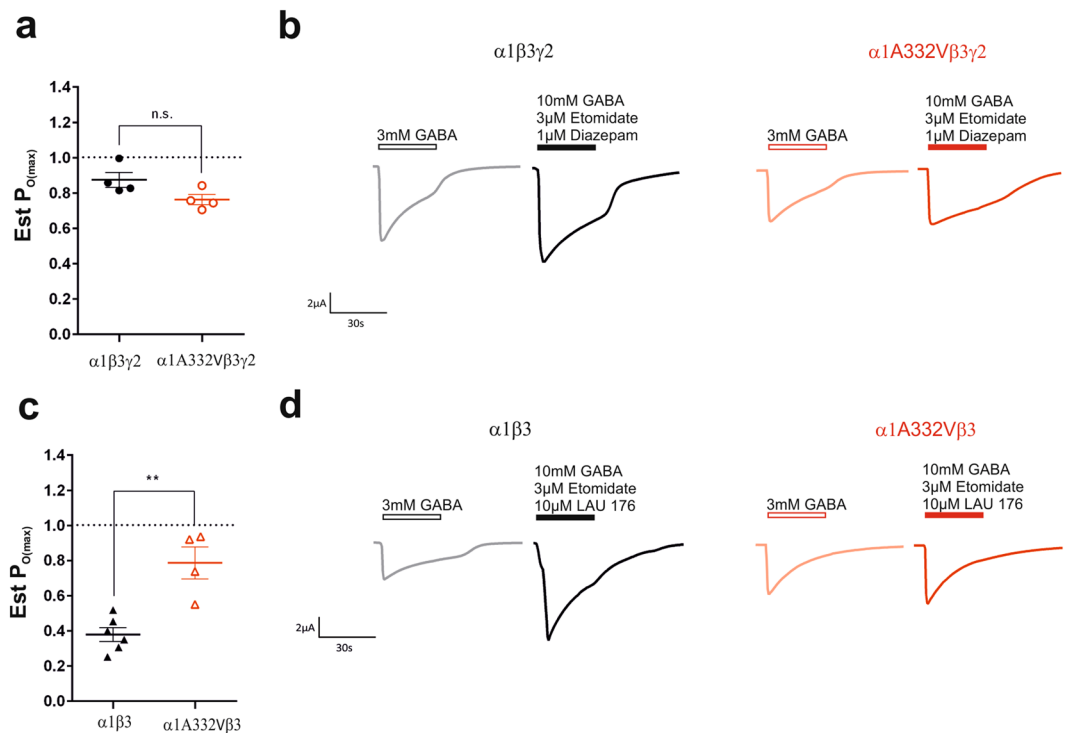


Figure 5. (a) Est. $P_{O(max)}$ values of $\alpha 1\beta 3\gamma 2$ and $\alpha 1A332V\beta 3\gamma 2$ receptors. The values were determined by dividing the current elicited by 3 mM GABA by the current elicited by 10 mM GABA, 1 μ M diazepam, and 3 μ M etomidate and corrected for the reference 3 mM GABA current. Lines and error bars represent the mean \pm SEM of 4 individual cells. (b) Representative traces from electrophysiological recordings in $\alpha 1\beta 3\gamma 2$ and $\alpha 1A332V\beta 3\gamma 2$ receptors after application of reference 3 mM GABA and 10 mM GABA, 1 μ M diazepam, and 3 μ M etomidate, respectively. (c) Est. $P_{O(max)}$ values of $\alpha 1\beta 3$ and $\alpha 1A332V\beta 3$ receptors. The values were determined by dividing the current elicited by 3 mM GABA by the current elicited by 10 mM GABA, 10 μ M LAU 176, and 3 μ M etomidate and corrected for the reference 3 mM GABA current. Lines and error bars represent the mean \pm SEM of 4–6 individual cells. (d) Representative traces from electrophysiological recordings in $\alpha 1\beta 3$ and $\alpha 1A332V\beta 3$ receptors after application of reference 3 mM GABA and 10 mM GABA, 10 μ M LAU 176, and 3 μ M etomidate, respectively. Statistically significant differences were determined by two-tailed students *t*-test, where $p < 0.05$; ** $p < 0.01$.

The receptors with the mutated $\alpha 1$ subunit are activated to a greater extent at the same GABA concentration due to the left shift (Fig. 4), and thus, the extent of desensitization might just reflect this left shift³⁵. To clarify, we also compared extent of desensitization at comparable level of activation or % of I_{max} (Supplementary Figs. S7 and S8). The extent to which the mutated receptors desensitize is higher also at comparable activation level.

Additionally, as an approximate measure for charge transfer in a GABA elicited event, the area under the curve (AUC) was determined at 30 μ M and 1 mM GABA in all four receptor types (Fig. 7). The results revealed that at both concentrations the AUC of the binary mutated receptor is significantly smaller than the binary wild-type receptor. A significant difference at 30 μ M can be also observed in $\alpha 1\beta 3\gamma 2$ and $\alpha 1A332V\beta 3\gamma 2$ receptors, whereas at 1 mM no difference is seen (Fig. 7).

Discussion

The identification of a - hitherto unreported - variant of unknown significance in a known disease associated gene is a frequently encountered result during clinical exome sequencing in infants with a suspected hereditary condition. Like in the case described in this paper, segregation analysis in healthy parents can determine whether the variant arose *de novo* and therefore represents formally a good candidate for being the disease-causing variant. Algorithms for predicting the probability whether a missense variant introduces a pathogenic amino acid exchange, such as MutationTaster or CADD, have evolved into powerful tools to streamline the process of assessing the significance of a novel variant^{25–27}. However, without functional studies, there will always be at least some degree of uncertainty in the final assessment. In the case reported here, the severe early-onset clinical manifestation of the affected individual prompted us to investigate the functional consequence of the identified variant (A332V).

A332V is localised in helix 3 of the transmembrane domain (TMD) of the $\alpha 1$ subunit. The TMD is highly conserved among different GABA_A receptor subunits and even within the Cys-loop receptor family: nAChR, 5-HT_{3A}R, glycine receptors and even bacterial homologues show extremely high structural conservation on a basis of as little as about 15% sequence identity¹⁷. Consistent with this, many variants in the TMD cause a molecular phenotype that can range from altered channel properties with regular expression to reduced functional

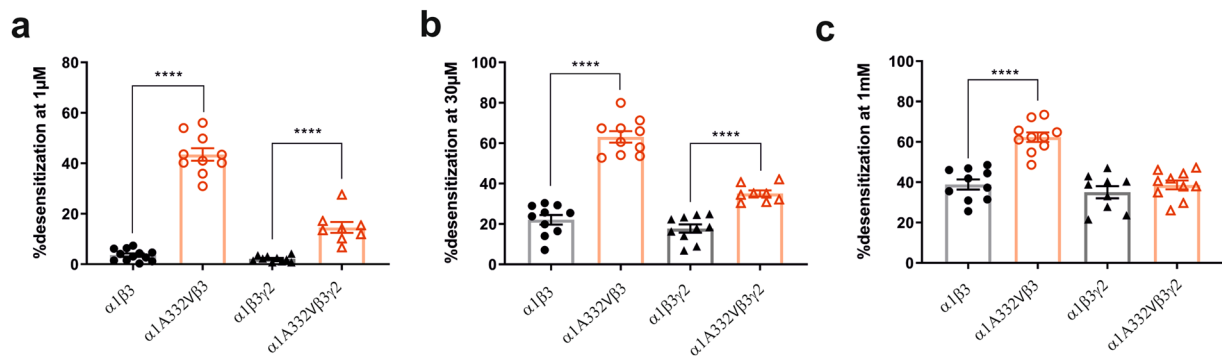


Figure 6. Extent of desensitization of wild-type and mutated receptors. The extent of desensitization was determined at 1 μM (a), 30 μM (b) and 1 mM GABA (c) as described in the methods (peak to 15 s) in all four receptor types. Statistically significant differences were determined by two-tailed students *t*-test, where $p < 0.05$; **** $p < 0.0001$. Bars are presented as mean \pm SEM. A comparison based on comparable level of activation, rather than on GABA concentration, is provided in Supplementary Fig. S7, while representative traces are depicted in Supplementary Fig. S8.

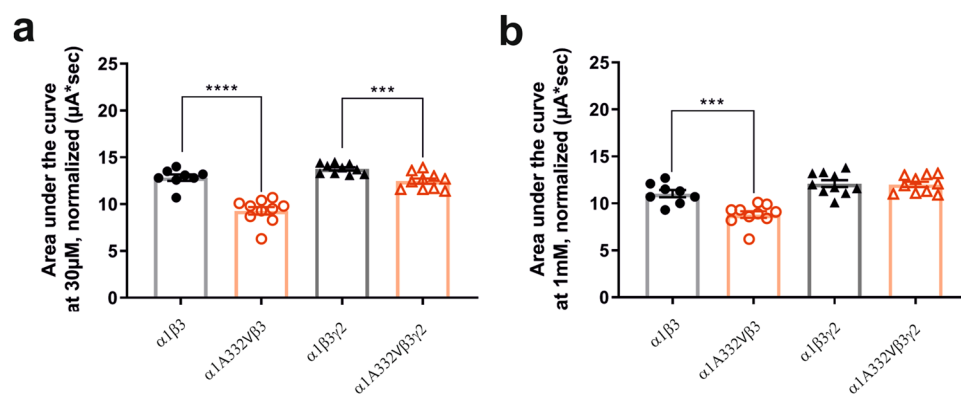


Figure 7. Area under the curve of wild-type and mutated receptors. Area under the curve was calculated at 30 μM (a) and 1 mM GABA (b) in all four receptor types. Statistically significant differences were determined by two-tailed students *t*-test, where $p < 0.05$; *** $p < 0.001$; **** $p < 0.0001$. Bars are presented as mean \pm SEM.

expression due to misfolding or protein retention in the ER^{19,20}. The case of $\alpha 1A332D$ has been studied in considerable detail. In this case, ER retention (likely due to misfolding) results in very low receptor expression, and thus, a clear “loss of function” phenotype.

Here we performed an *in vitro* characterisation of the A332V variant. Expression and forward trafficking to the cell surface appears unchanged in HEK293 cells as evidenced by western blot results indicating that the amount of total $\alpha 1$ protein is similar to wild-type, and further supported by immunocytochemical stainings indicating regular trafficking to the cell surface.

The radioligand displacement assays in HEK293 cells indicate that the $\alpha - \gamma$ interface in recombinant $\alpha 1A332V\beta 3\gamma 2$ receptors is regularly built because the binding of benzodiazepines to the $\alpha 1(+)\gamma 2(-)$ interface is not impaired. However, the IC_{50} values of diazepam-displacement differ by one order of magnitude, with diazepam binding with higher affinity to the mutated receptor. Nevertheless, this shift might not be pharmacologically relevant *in vivo*.

Functional analysis was performed in *Xenopus laevis* oocytes, using cells injected with $\alpha 1A332V$ and $\beta 3$ mRNA as well as cells with the ternary $\alpha 1A332V, \beta 3$ and $\gamma 2$ combination. The former cells express an extrasynaptic receptor subtype, while the ternary mix of mRNA yields mixed pools $\alpha\beta$ and $\alpha\beta\gamma$ receptors^{36,37}. Robust GABA elicited currents indicate also in this recombinant system regular expression and forward trafficking.

The mutated $\alpha 1$ subunit confers changes in GABA potency, where the mutated subunit induces an apparent left shift of the GABA dose response compared to wild-type for both tested subunit combinations. We sought to also investigate channel opening and desensitization characteristics. Since the maximum current amplitude may be underestimated by application of GABA alone, we estimated the maximum open probability of wild-type and mutated receptors as described previously^{29,31,32}. Similar to Absalom *et al.* we observed a high $Est.P_{O(max)}$ in wild-type γ -containing receptors. For the mutated receptors no significant difference to WT was observed. For the case of $\alpha 1\beta 3$ receptors GABA does not seem to be a full agonist, since the application of established allosteric modulators resulted in more pronounced enhancement of the current elicited by a saturating GABA

concentration. In contrast, this increase in efficacy is not observed in $\alpha 1A332V\beta 3$ receptors resulting in a significantly higher $Est.P_{O(max)}$ compared to wild-type receptors in response to a saturating GABA concentration. $\alpha 1\beta 3$ receptors are considered to contribute to an extrasynaptic pool of receptors which mediate tonic inhibition³⁷. Typically, extrasynaptic receptors are activated by low concentrations of ambient GABA, causing long lasting currents which tend to be smaller than currents produced by synaptic receptors. A characteristic of this pool of receptors is that due to their different intrinsic properties compared to synaptic receptors they can confer seemingly magnified modulatory efficacy, an outcome often observed with several allosteric modulators³¹. It is interesting to note that the mutation impacts on GABA efficacy for $\alpha 1A332V\beta 3$, but not for $\alpha 1A332V\beta 3\gamma 2$.

Receptor desensitization is also altered. Due to the faster desensitization, the total charge transfer per GABA elicited event is reduced as evidenced by the area under the curve of the whole cell current traces. Comparing desensitization levels at comparable levels of activation indicates that the mutant accelerates desensitization in both the tested subunit combinations. This could be rationalised from the proximity of the mutation to the desensitization gate in the lower TMD³⁸.

In summary, subunit folding, receptor assembly and forward trafficking appears to be unchanged in HEK cells and *Xenopus* oocytes. In contrast, channel properties are changed considerably, and in ways that depend on subunit composition. The $\alpha 1$ subunit contributes to multiple receptor subtypes expressed by neurons, including phasically active $\alpha 1\beta 2$ and tonically active $\alpha 1\beta$, $\alpha 1\beta\delta$ or $\alpha 1\alpha 6\beta\delta$ receptors, just to name a few. The altered GABA efficacy, sensitivity and desensitization characteristics will impact on both phasic and tonic currents in neurons in ways that cannot be predicted based on the data presented here, because the actual impact of increased sensitivity at low GABA concentrations and accelerated desensitization already at moderate concentrations will depend on the precise neuronal events: At extrasynaptic receptors the influence of desensitization may lower the effective inhibitory tone in spite of the higher GABA potency, and thus contribute to a shift in seizure threshold. On the other hand, the left shifted GABA response may lead to altered phasic inhibition, where inhibitory postsynaptic events may occur excessively or due to ambient GABA.

A332V should be seen as a “molecular change of function” variant which induces an increased sensitivity to low GABA concentrations in combination with accelerated desensitization and some impact on agonist efficacy that is more pronounced in $\alpha 1\beta 3$ receptors. What can be extrapolated to the possible role of the missense variant in the heterozygous carrier? Here we tested receptors in which all subunits are either wild-type, or mutated. It has been shown recently that functional alterations can be remarkably different if a pentamer contains one wild-type and one mutated subunit, and that even the position of the mutated subunit severely impacts on receptor function²⁹. Given that the affected individual is heterozygous, conclusions from the molecular findings here to the onset and development of symptoms are impossible. The net effects of the heterozygous variant can be investigated in more detail only in transgenic animals, or patient derived organoid or spheroid cell culture models. To discern under which circumstances the mutant will contribute to reduced, or enhanced GABA responses requires a broad variety of experiments with *in vitro* and *in vivo* preparations that are able to recapitulate the presence of one wild type and one mutated gene, the wide diversity of $\alpha 1$ containing receptor species, and their temporal expression patterns in the time after birth when the *GABRA1* expression gets gradually upregulated.

In spite of all these limitations, it still is possible to speculate on possible mechanisms by which the observed molecular phenotype could induce some aspects of the syndrome and specifically could be driving the seizure phenotype. The onset of symptoms can be seen as highly consistent with the postnatal up-regulation in *GABRA1* expression in the brain. Seizures are indicative of an excitation/inhibition imbalance. A direct effect by a dramatic loss of function at the receptor level cannot be predicted based on the *in vitro* data, while some mixture of loss and gain of function would be plausible. A secondary loss of receptors due to enhanced internalization that develops over time would be a plausible candidate in case the gain of function occurs as a dominant consequence of the altered mix of molecular properties. In fact, if $GABA_A$ receptors are chronically stimulated with agonists or positive modulators, increased receptor turnover and subsequent changes in gene expression have been consistently observed, suggesting that excessive channel activity leads to compensatory changes³⁹. The left shifted GABA response we observe here could thus drive a secondary downregulation of the affected and other subunits. This hypothesis is probably the most plausible, but impossible to validate with *in vitro* experiments.

Overall, we can conclude that the A332V missense variant in the $\alpha 1$ subunit impacts receptor function at the level of GABA and benzodiazepine function, and on desensitization characteristics, which might drive a broad range of adaptive cellular responses.

Methods

All methods were carried out in accordance with relevant guidelines and regulations of the Medical University of Vienna, Austria.

Clinical information. Clinical information and family history were collected using records submitted by the referring clinicians. Informed consent was obtained from the patient’s parents in accordance with the regulations of local ethics review boards of the Medical University of Vienna, Austria.

Next-generation sequencing. Exome sequencing was performed in 2014 from a DNA sample isolated from peripheral blood of the affected individual. Libraries were constructed using the Agilent SureSelect All Exon V5 kit (Agilent, Santa Clara, CA, USA) and sequenced using the Illumina HiSeq sequencing system (Illumina, San Diego, CA, USA) with 100 bp paired-end reads. All library preparation and sequencing steps were performed at GATC Biotech AG (now: Eurofins Genomics; Constance, Germany). Sequences were analysed at the Neuromuscular Research Department using an in-house developed bioinformatics pipeline starting from fastq files. In brief, reads were mapped to the human genome reference sequence (build hg19) using the BWA-MEM algorithm⁴⁰. Within the targeted coding exons, the average depth of coverage was 60-fold with 90%

of target sequence covered at least 10-fold. Variant calling was performed using the GATK Haplotype Caller⁴¹. Variant filtration was performed with ANNOVAR and exported to Excel spreadsheets⁴². The final data analysis was done using minor allele frequencies from reference datasets (1k genomes, ESP, ExAC, gnomAD) for genes known to be causatively related to epileptic encephalopathies, which revealed a so far unreported variant in the *GABRA1* (gamma-aminobutyric acid type A receptor alpha1 subunit) gene: hg19 chr5:g.161322810C > T; NM_000806.5:c.995C > T p.(Ala332Val). Different algorithms were used to predict potential pathogenicity of the identified variant, including MutationTaster ($P > 0.999$) and CADD (Phred = 34)^{25–27}.

Segregation was analysed by PCR (forward primer: 5'-TTTCCTTTTGTTC AAGTAGGCTGT-3'; reverse primer: 5'-TTCTGCATACTCCATCCAATACC-3', for amplifying a 390 bp-fragment comprising of exon 10 and flanking intron boundaries), followed by conventional Sanger DNA sequencing in the affected individual and both parents.

Cloning. Cloning of the mutated human $\alpha 1$ cDNA was performed using a human $\alpha 1$ -pCI construct and the Q5 Site-Directed Mutagenesis Kit (New England Biolabs) following manufacturer's instructions with the following primers: 5'-ATTGAGTTTGT CACAGTAAC-3' and 5'-CAGAGCTGAGAACACAAAG-3'. The small letter indicates the base changed by mutagenesis leading to an exchange of alanine at position 332 to valine in the protein.

HEK293 cell transfection and radioligand binding. Transfection of HEK293 cells with a combination of human wild-type or mutant $\alpha 1\beta 3\gamma 2$ cDNAs (ratio 1:1:5) and displacement of radioactively labelled ³H-flunitrazepam with different concentrations of diazepam (from 1 nM, 3 nM, 10 nM, 33 nM, 100 nM, 333 nM, 1 μ M to 3 μ M) was performed as described previously⁴³.

Membrane preparation and protein determination. Membranes of HEK293 cells transfected with either wild-type or mutant human $\alpha 1\beta 3\gamma 2$ cDNAs (ratio: 1:1:5) were prepared as described previously⁴⁴. Protein concentrations were determined using the Pierce™ BCA protein assay kit (ThermoFisher Scientific) following manufacturer's protocol.

SDS-PAGE, Western blot and fluorescence detection. Samples for western blot were prepared as described previously⁴⁴. 20 μ g of samples and 0.5 μ l of protein marker were separated on a gel according to standard Laemmli method. Gels were blotted semi-dry on pre-wetted polyvinylidene fluoride membranes. Membranes were blocked in blocking buffer (5% milk/PBS without Tween 20) o/n at 4 °C. They were then incubated with 0.5 μ g/ml primary antibody in blocking buffer (5% milk/PBST) for 24 h at 4 °C⁴⁵. Afterwards, membranes were incubated with 0.5 μ g/ml primary anti-GAPDH mouse antibody in blocking buffer for 24 h at 4 °C and washed 4 \times 5 min with washing buffer (1.5% milk/PBST). Membranes were incubated with secondary antibodies diluted 1:10 000 in washing buffer (Alexa Fluor® 680-conjugated goat anti-mouse light chain, Jackson ImmunoResearch and IRDye® 800CW-conjugated donkey anti-rabbit, LI-COR® Biosciences) for 1 h at room temperature. After incubation, membranes were washed again 4 \times 5 min with washing buffer. Membranes were scanned at 700 and 800 nm using the Odyssey System (LI-COR® Biosciences). Band intensities were analysed with the Image Studio software version 5.2 for Windows (LI-COR® Biosciences). A complete western blot is shown in Fig. 2b.

Immunocytochemistry. HEK293 cells transfected with a combination of human wild-type or mutant $\alpha 1\beta 3\gamma 2$ cDNAs (ratio 1:1:5) were fixed with fresh 4% PFA followed by 2x washing with 1x PBS. Cells were then incubated for 1 h at RT in blocking solution (10% normal donkey serum (NDS), 5% BSA, 0.3% Triton X-100/PBS). After blocking, the cells were treated with 0.65 μ g/ml primary antibody in buffer (5% NDS, 2% BSA, 0.3% Triton X-100/PBS) for 16 h at 4 °C⁴⁵. After washing the cells 3 \times 20 min in PBS, immunoreactivities were revealed using anti-rabbit (1:300) secondary antibodies (Jackson ImmunoResearch) conjugated with Cy3 fluorophores diluted in 2% BSA in PBS. Nuclei were stained with Hoechst. After the final washes (3 \times 40 min) the coverslips with the stained cells were mounted on microscopy glass slides with glycerol gelatine. Imaging was executed on a Zeiss 780LSM laser-scanning microscope and assembled in CorelDraw X7 (Corel Corporation).

Two-electrode voltage electrophysiology. All steps were performed as reported previously³³. In brief, cloned pCI vectors encoding for human GABA_A receptor subunits $\alpha 1$, $\alpha 1A332V$, $\beta 3$ and $\gamma 2$ were linearised, transcribed and purified in order to generate mRNA. For the microinjection, the RNA of the $\alpha 1/\alpha 1A332V$ - $\beta 3$ receptor combination was mixed at 1:1 ratio and for the $\alpha 1/\alpha 1A332V$ - $\beta 3\gamma 2$ receptor at 1:1:5 ratio with a final concentration of 56 ng/ μ l. Mature *Xenopus laevis* oocytes were obtained in full accordance with all rules of the Austrian animal protection law and the Austrian animal experiment by-laws which implement European Directive 2010/63/EU into Austrian law. Stage 5–6 oocytes were then digested and defolliculated as described previously³³. The cells were injected with an aqueous solution of mRNA (2.8 ng/oocyte) and incubated for 2–3 days at 18 °C before electrophysiological recordings. For current measurements the oocytes were impaled with two microelectrodes (1–3 M Ω) filled with 2 M KCl. The oocytes were constantly washed by a flow of 6 ml/min NDE (96 mM NaCl; 2 mM KCl; 1 mM MgCl₂ \times 6H₂O; 5 mM Hepes; 1.8 mM CaCl₂ \times 2H₂O; pH 7.5) that could be switched to NDE containing GABA. GABA was applied for 20 seconds and between two applications oocytes were washed in NDE for up to 15 min to ensure full recovery from desensitization.

For estimating the maximal open probability Est. $P_{O(max)}$ experiments were conducted similar to Absalom *et al.*²⁹. 3 mM GABA was used as a reference concentration and was applied two times at the beginning of the experiment. For $\alpha\beta$ containing receptors, a solution consisting of 10 mM GABA, 3 μ M etomidate and 10 μ M LAU 176 was applied for 30 seconds^{33,34}. For $\alpha\beta\gamma$ containing receptors 1 μ M diazepam was used instead of LAU 176. As shown in Absalom *et al.*, cells were washed 10–15 min between the applications. Peak currents were normalised to the mean of the two 3 mM GABA applications. All recordings were performed at room temperature at a

holding potential of -60 mV using a Dagan TEV-200A two-electrode voltage clamp (Dagan Corporation). Data were digitised, recorded and measured using an Axon Digidata 1550 low-noise data acquisition system (Axon Instruments). Data acquisition was performed using pCLAMP v.10.5 (Molecular Devices™).

Data analysis. For the radioligand binding assays, IC_{50} values were derived from the displacement curve calculated as nonlinear fit with a variable hill slope using the following formula and bottom = 0%, top = 100%:

$$Y = \text{Bottom} + \frac{\text{Top} - \text{Bottom}}{1 + 10^{((\text{Log}IC_{50} - X) * \text{Hillslope})}}$$

Data obtained from electrophysiological experiments were analysed using GraphPad Prism v.7.00 and plotted as concentration-response curves. These curves were normalised and fitted by non-linear regression analysis to the equation, where $\log EC_{50}$ is the X value when the response is half way between top and bottom y values, and nH is the Hill coefficient.

$$Y = \text{Bottom} + \frac{\text{Top} - \text{Bottom}}{1 + 10^{((\text{Log}EC_{50} - X) * \text{Hillslope})}}$$

Data are given as mean \pm SEM from at least five oocytes of two and more oocyte batches.

The desensitization of the receptor and the respective area under the curve (AUC) for each trace were calculated for the region between the maximal current amplitude and the residual current amplitude reached 15 sec after maximum. Desensitization was measured at currents induced by $1 \mu\text{M}$, $30 \mu\text{M}$ and 1mM GABA for all receptors. The extent of desensitization was determined as given:

$$\text{Desensitization}[\%] = \left(1 - \frac{I_{\text{residual}}}{I_{\text{peak}}} \right) \times 100$$

I_{peak} is the agonist-induced peak current and I_{residual} the residual of this current 15 seconds after the peak amplitude⁴⁶.

For calculating the area under the curve, currents induced by $30 \mu\text{M}$ and 1mM GABA in all four receptor types were taken into account. The traces were first normalised so that all points of the current response span the range 0 to 1. The normalisation function is as follows, where y_{min} is the smallest and y_{max} is the largest value in the trace:

$$f(y) = - \left(1 - \frac{(y - y_{\text{min}})}{(y_{\text{max}} - y_{\text{min}})} \right)$$

The areas under the curve confined by the baseline, the normalised maximum and the normalised residual current 15 sec after maximum were determined by the “Area” function of Clampfit 10.7.03.

Statistical significance for all analyses was calculated using a one sample *t*-test. P-values of <0.05 were accepted as statistically significant.

Data availability

The datasets generated and/or analysed during the current study are available from the corresponding author upon request.

Received: 12 August 2019; Accepted: 28 January 2020;

Published online: 11 February 2020

References

- Olsen, R. W. & Sieghart, W. International Union of Pharmacology. LXX. Subtypes of gamma-aminobutyric acid(A) receptors: classification on the basis of subunit composition, pharmacology, and function. *Update. Pharmacol. Rev.* **60**, 243–260 (2008).
- Kilb, W. Development of the GABAergic system from birth to adolescence. *Neuroscientist* **18**, 613–630 (2012).
- Zeilhofer, H. U., Wildner, H. & Yevenes, G. E. Fast synaptic inhibition in spinal sensory processing and pain control. *Physiol. Rev.* **92**, 193–235 (2012).
- Araujo, F. *et al.* Molecular and pharmacological characterization of native cortical gamma-aminobutyric acidA receptors containing both alpha1 and alpha3 subunits. *J. Biol. Chem.* **271**, 27902–27911 (1996).
- Benke, D. *et al.* Analysis of the presence and abundance of GABAA receptors containing two different types of alpha subunits in murine brain using point-mutated alpha subunits. *J Biol Chem* **279** (2004).
- Jechlinger, M., Pelz, R., Tretter, V., Klausberger, T. & Sieghart, W. Subunit composition and quantitative importance of hetero-oligomeric receptors: GABAA receptors containing alpha6 subunits. *J. Neurosci.* **18**, 2449–2457 (1998).
- Laurie, D. J., Wisden, W. & Seeburg, P. H. The distribution of thirteen GABAA receptor subunit mRNAs in the rat brain. III. Embryonic and postnatal development. *J. Neurosci.* **12**, 4151–4172 (1992).
- Wang, D. D. & Kriegstein, A. R. Defining the role of GABA in cortical development. *J. Physiol.* **587**, 1873–1879 (2009).
- Wu, C. & Sun, D. GABA receptors in brain development, function, and injury. *Metab. Brain Dis.* **30**, 367–379 (2015).
- Tyzio, R. *et al.* Maternal oxytocin triggers a transient inhibitory switch in GABA signaling in the fetal brain during delivery. *Sci.* **314**, 1788–1792 (2006).
- Fritschy, J. M., Paysan, J., Enna, A. & Mohler, H. Switch in the expression of rat GABAA-receptor subtypes during postnatal development: an immunohistochemical study. *J. Neurosci.* **14**, 5302–5324 (1994).
- Lopez-Tellez, J. F. *et al.* Postnatal development of the alpha1 containing GABAA receptor subunit in rat hippocampus. *Brain Res. Dev. Brain Res* **148**, 129–141 (2004).
- McKernan, R. M., Cox, P., Gillard, N. P. & Whiting, P. Differential expression of GABAA receptor alpha-subunits in rat brain during development. *FEBS Lett.* **286**, 44–46 (1991).
- Duncan, C. E. *et al.* Prefrontal GABA(A) receptor alpha-subunit expression in normal postnatal human development and schizophrenia. *J. Psychiatr. Res.* **44**, 673–681 (2010).

15. Pinto, J. G. A., Hornby, K. R., Jones, D. G. & Murphy, K. M. Developmental changes in GABAergic mechanisms in human visual cortex across the lifespan. *Front. Cell Neurosci.* **4**, 16–16 (2010).
16. Ernst, M., Steudle, F. & Bampali, K. In *eLS* (John Wiley & Sons, Ltd, 2001).
17. Puthenkalam, R. *et al.* Structural Studies of GABA-A receptor binding sites: Which experimental structure tells us what? *Front Mol Neurosci* **9** (2016).
18. Hernandez, C. C. & Macdonald, R. L. A structural look at GABAA receptor mutations linked to epilepsy syndromes. *Brain Res.* **1714**, 234–247 (2019).
19. Cossette, P. *et al.* Mutation of GABRA1 in an autosomal dominant form of juvenile myoclonic epilepsy. *Nat. Genet.* **31**, 184–189 (2002).
20. Hirose, S. Mutant GABA(A) receptor subunits in genetic (idiopathic) epilepsy. *Prog. Brain Res.* **213**, 55–85 (2014).
21. Maljevic, S. *et al.* A mutation in the GABA(A) receptor alpha(1)-subunit is associated with absence epilepsy. *Ann. Neurol.* **59**, 983–987 (2006).
22. Johannesen, K. *et al.* Phenotypic spectrum of GABRA1: From generalized epilepsies to severe epileptic encephalopathies. *Neurol.* **87**, 1140–1151 (2016).
23. Gallagher, M. J., Ding, L., Maheshwari, A. & Macdonald, R. L. The GABAA receptor alpha1 subunit epilepsy mutation A322D inhibits transmembrane helix formation and causes proteasomal degradation. *Proc. Natl Acad. Sci. USA* **104**, 12999–13004 (2007).
24. Karczewski, K. J. *et al.* Variation across 141,456 human exomes and genomes reveals the spectrum of loss-of-function intolerance across human protein-coding genes. *bioRxiv*, 531210 (2019).
25. Kircher, M., Witten, D. M., Jain, P., O’Roak, B. J. & Cooper, G. M. A general framework for estimating the relative pathogenicity of human genetic variants. *Nat. Genet.* **46**, 310–315 (2014).
26. Rentzsch, P., Witten, D., Cooper, G. M., Shendure, J. & Kircher, M. CADD: predicting the deleteriousness of variants throughout the human genome. *Nucleic Acids Res.* **47**, D886–d894 (2019).
27. Schwarz, J. M., Cooper, D. N., Schuelke, M. & Seelow, D. MutationTaster2: mutation prediction for the deep-sequencing age. *Nat. Methods* **11**, 361 (2014).
28. Sieghart, W. Allosteric modulation of GABAA receptors via multiple drug-binding sites. *Adv. Pharmacol.* **72**, 53–96 (2015).
29. Absalom, N. L. *et al.* Functional genomics of epilepsy-associated mutations in the GABAA receptor subunits reveal that one mutation impairs function and two are catastrophic. *J. Biol. Chem.* **294**, 6157–6171 (2019).
30. Eaton, M. M. *et al.* Gamma-aminobutyric acid type A alpha4, beta2, and delta subunits assemble to produce more than one functionally distinct receptor type. *Mol. Pharmacol.* **86**, 647–656 (2014).
31. Ahring, P. K. *et al.* A pharmacological assessment of agonists and modulators at alpha4beta2gamma2 and alpha4beta2delta GABAA receptors: The challenge in comparing apples with oranges. *Pharmacol. Res.* **111**, 563–576 (2016).
32. Feng, H. J., Jounaidi, Y., Haburcak, M., Yang, X. & Forman, S. A. Etomidate produces similar allosteric modulation in $\alpha 1\beta 3\delta$ and $\alpha 1\beta 3\gamma 2\text{L}$ GABA(A) receptors. *Br. J. Pharmacol.* **171**, 789–798 (2014).
33. Simeone, X. *et al.* Molecular tools for GABAA receptors: High affinity ligands for $\beta 1$ -containing subtypes. *Sci. Rep.* **7**, 5674 (2017).
34. Varagic, Z. *et al.* Identification of novel positive allosteric modulators and null modulators at the GABAA receptor alpha+beta-interface. *Br. J. Pharmacol.* **169**, 371–383 (2013).
35. Germann, A. L. *et al.* Steady-state activation and modulation of the synaptic-type alpha1beta2gamma2L GABAA receptor by combinations of physiological and clinical ligands. *Physiol. Rep.* **7**, e14230 (2019).
36. Baburin, I. *et al.* Estimating the efficiency of benzodiazepines on GABA(A) receptors comprising gamma1 or gamma2 subunits. *Br. J. Pharmacol.* **155**, 424–433 (2008).
37. Mortensen, M. & Smart, T. G. Extrasynaptic alphabeta subunit GABAA receptors on rat hippocampal pyramidal neurons. *J. Physiol.* **577**, 841–856 (2006).
38. Scott, S. & Aricescu, A. R. A structural perspective on GABAA receptor pharmacology. *Curr. Opin. Struct. Biol.* **54**, 189–197 (2019).
39. Gravielle, M. C. Regulation of GABAA receptors by prolonged exposure to endogenous and exogenous ligands. *Neurochem. Int.* **118**, 96–104 (2018).
40. Li, H. Aligning sequence reads, clone sequences and assembly contigs with BWA-MEM. *ArXiv* **1303** (2013).
41. Van der Auwera, G. A. *et al.* From FastQ data to high confidence variant calls: the Genome Analysis Toolkit best practices pipeline. *Curr Protoc Bioinformatics* **43**, 11.10.11–33 (2013).
42. Wang, K., Li, M. & Hakonarson, H. ANNOVAR: functional annotation of genetic variants from high-throughput sequencing data. *Nucleic Acids Res.* **38**, e164 (2010).
43. Stamenic, T. T. *et al.* Ester to amide substitution improves selectivity, efficacy and kinetic behavior of a benzodiazepine positive modulator of GABAA receptors containing the alpha5 subunit. *Eur. J. Pharmacol.* **791**, 433–443 (2016).
44. David, R. *et al.* Biochemical and functional properties of distinct nicotinic acetylcholine receptors in the superior cervical ganglion of mice with targeted deletions of nAChR subunit genes. *Eur. J. Neurosci.* **31**, 978–993 (2010).
45. Mossier, B., Togel, M., Fuchs, K. & Sieghart, W. Immunoaffinity purification of gamma-aminobutyric acidA (GABAA) receptors containing gamma 1-subunits. Evidence for the presence of a single type of gamma-subunit in GABAA receptors. *J. Biol. Chem.* **269**, 25777–25782 (1994).
46. Gielen, M., Thomas, P. & Smart, T. G. The desensitization gate of inhibitory Cys-loop receptors. *Nat. Commun.* **6**, 6829 (2015).
47. Masiulis, S. *et al.* GABAA receptor signalling mechanisms revealed by structural pharmacology. *Nat.* **565**, 454–459 (2019).

Acknowledgements

The authors would like to thank Jure Fabjan for his assistance with data analysis and for constructive discussions. The work was funded by the Austrian Science Fund grant W1232 MolTag.

Author contributions

M.E., W.M.S., F.S. and S.R. conceived the study. P.S. supervised experiments. F.S., S.R. and X.S. planned and performed experiments. F.S., S.R., X.S. and K.B. performed data analysis. Z.R. and E.H. collected clinical information. F.S., S.R., K.B., W.M.S. and M.E. wrote the manuscript.

Competing interests

The authors declare no competing interests.

Additional information

Supplementary information is available for this paper at <https://doi.org/10.1038/s41598-020-59323-6>.

Correspondence and requests for materials should be addressed to K.B.

Reprints and permissions information is available at www.nature.com/reprints.

Publisher's note Springer Nature remains neutral with regard to jurisdictional claims in published maps and institutional affiliations.



Open Access This article is licensed under a Creative Commons Attribution 4.0 International License, which permits use, sharing, adaptation, distribution and reproduction in any medium or format, as long as you give appropriate credit to the original author(s) and the source, provide a link to the Creative Commons license, and indicate if changes were made. The images or other third party material in this article are included in the article's Creative Commons license, unless indicated otherwise in a credit line to the material. If material is not included in the article's Creative Commons license and your intended use is not permitted by statutory regulation or exceeds the permitted use, you will need to obtain permission directly from the copyright holder. To view a copy of this license, visit <http://creativecommons.org/licenses/by/4.0/>.

© The Author(s) 2020